Published in final edited form as:
J Magn Reson Imaging. 2009 March ; 29(3): 583–587. doi:10.1002/jmri.21702.

A Phase-Contrast MRI-based Elastography Technique Detects Early Hypertensive Changes in ex-vivo Porcine Aortic Wall

David A. Woodrum, MD/PhD[1], **Joerg Herrmann, MD**[2], **Amir Lerman, MD**[2], **Anthony J. Romano, PhD**[3], **Lilach O. Lerman, MD/PhD**[4], and **Richard L. Ehman, MD**[1]

[1]Radiology Department, Mayo Clinic, Rochester, Minnesota, USA

[2]Cardiology Department, Mayo Clinic, Rochester, Minnesota, USA

[3]Naval Research Laboratory, Washington, DC, USA

[4]Nephrology and Hypertension, Department, Mayo Clinic, Rochester, Minnesota, USA

Abstract

Purpose—To measure the elastic properties of ex-vivo porcine aortas in control and hypertensive groups using a phase contrast MRI-based elastography technique.

Materials and Methods—Female domestic pigs were randomized to a normal control group (N; n=5) or a renovascular hypertension group (HT; n=5) for the duration of 3 months. Mean arterial pressure was significantly higher in the hypertension group than in the control group (173 ± 12 vs. 115 ± 11 mmHg, $p \leq 0.05$). The animals were euthanized after 3 months of hypertension and abdominal aortas harvested. The ex-vivo aortic samples were then examined using a phase contrast MRI-based elastography technique.

Results—The Young's modulus-wall thickness product, a reflection of vascular stiffness, was significantly higher in the hypertension group than in the control group (0.571 ± 0.080 vs. 0.419 ± 0.026, $p<0.05$). Histological analysis and staining confirmed increased intima-media thickness and collagen content in the hypertensive aorta, while elastin staining showed no difference.

Conclusion—The current study shows that MR elastography offers a method to study the physiologic changes in the arterial wall secondary to early hypertension.

Keywords

MRI; Elastography; Aorta

Hypertension is a major risk factor associated with atherosclerosis contributing to a greater increase in cardiac events. It has been shown to contribute to fundamental pathologic processes such as systemic remodeling of blood vessel walls, changes in mural extracellular matrix, and abnormal smooth muscle tone contributing to increased wall stiffness (1). This is important because the elastic and muscular properties of the vascular wall determine the propagation of the pulse wave generated with every beat of the heart. The central arteries, i.e. the aorta and its branches, are rich in the elastic components, which smooth out blood flow and pressure (so-called “Windkessel effect”) (2). On the contrary, the muscular elements predominate in the peripheral arteries and determine vascular resistance. Advancing age and systemic arterial hypertension change the structural relaxation properties of the central arteries much more than the muscular arteries by increasing the collagen-

Corresponding Author: David A. Woodrum, 200 First Street SW, Rochester, MN 55905, Phone: 507-255-7131, Fax: 507-255-7872, Woodrum.david@mayo.edu.

elastin ratio (3). This leads to a reduction in the elasticity of the central arteries as well as a reduction of the Windkessel effects with an acceleration of the pulse wave and its reflection in the periphery (2,4). The hemodynamic consequences are augmentation of systolic rather than diastolic blood pressure with an increase in the systolic work-load on the heart and a decrease in the diastolic perfusion of the heart (3). Hence, loss of elasticity of the central conduits over time leads to left ventricular hypertrophy, myocardial ischemia, and increased degenerative changes of the arterial system, thereby adding an important dimension to cardiovascular morbidity and mortality (3,5). Indeed, increased blood pressure is an important determinant of pulse wave velocity, which has been utilized as an index of arterial stiffness (6).

Different methodologies have tried to assess vascular stiffness such as analysis of pulse wave velocity (PWV), arterial pressure waveform analysis, and relating change in arterial diameter (or area) to distending pressure. Even though a number of tonometry- and ultrasound-based devices within these three categories are easy to use, their indirect estimate of elasticity, the data bias, and the reduced validity relating to operator experience have been outlined as potential barriers to widespread reliable use (7,8). Hence, while recognized to be an important element for some time, direct measurement of aortic elasticity has not become readily available and no diagnostic gold standard has been established so far. Two MR-based methods, phase contrast MRI and MR elastography, with the potential for non-invasive study of the arterial wall have emerged. Phase contrast MR imaging has been studied in a normotensive porcine model and given good results (9). The other method being studied utilizes a phase contrast MRI-based elastography technique (7).

The developed phase contrast MRI-based elastography technique can image micron-amplitude propagating waves induced in the walls of blood vessels by harmonic mechanical stimulation at acoustic frequencies and can be used to quantify vascular wall stiffness (10-12). Additionally, it is also able to determine very small changes in wall thickness and elasticity as determined in model systems (10). Arteries are naturally conducive to this methodology due to the natural wave guide conduction properties (10,13,14). In this study, we therefore hypothesized that early changes in arterial wall elasticity, secondary to hypertension, can be visualized and measured using this novel technique in a previously characterized animal model (15).

Methods

Hypertensive Porcine Model

The current study was approved by the Institutional Animal Care and Use Committee, and all procedures were in line with the NIH Guidelines. Three month-old female domestic pigs were randomized to two different three-month study groups. The first (control) group included pigs that were observed with no additional intervention (N, n=5). The second (hypertensive) group comprised pigs in which systemic arterial hypertension was induced by placement of a copper-stent in the left renal artery leading to unilateral renal artery stenosis, as previously established (HT, n=5) (15-17). Continuous blood pressure measurements were obtained in all animals by use of a telemetry system (PhysioTel, Data Sciences) implanted at baseline in the left femoral artery. Mean arterial pressure was recorded at 5-minute intervals and averaged for each 24-hour period. At the end of the study period, the pigs were euthanized with a lethal injection of sodium pentobarbitol (100 mg/kg IV; Sleepaway, Fort Dodge Laboratories). Porcine abdominal aortas were harvested immediately after euthanasia and placed in a Krebs solution. Separate aortic samples were subjected to formalin fixation and paraffin embedding for histological analyses. The connective tissue was removed from the outside of the aorta with side branches tied off. The diameter of the porcine aortas was approximately 1.5-1.8 cm with a length of approximately 30 cm. Each ex-vivo aorta was

inserted into a MR head coil under static pressure (approximately 115mm of mercury) filled with normal saline (0.9% NaCl). An electromechanical impulse generator was applied to the vessel wall

Magnetic Resonance Imaging Technique

For all experiments, imaging was performed on a 1.5 T whole body imager (GE Medical Systems, Waukesha, WI, USA) utilizing a transmit and receive head coil. The imaging technique incorporated oscillating, motion sensitizing field gradients that were synchronized with the propagating mechanical waves (8,9). Data acquisition parameters were: gradient echo acquisition, single coronal slice of 5 mm thickness, 100 ms repetition time (TR), 256 × 64 acquisition matrix which was interpolated to 256 × 256 matrix, 30 flip angle, and FOV of 20 cm. The porcine aorta (diameter 1.5-1.8 cm) was inserted into a MR head coil during imaging with an electromechanical impulse generator applied to the vessel wall. The imaging plane was along the longitudinal axis of the vessel. The impulse driver delivered a burst count of 8 cycles with 4 imaging time offsets obtained at 13-s intervals throughout a vibration cycle for each condition. The wavelengths were calculated by peak to peak measurement of the propagating longitudinal wave imaged within the arterial wall (Fig. 1a). The experiments were conducted using five impulse frequencies (100, 200, 300, 400 and 500 Hz). Post-processing assessment of the data consisted of directional filtering as described by Manduca et al. (18) to calculate exact wavelength (peak to peak distance). A minimum of a half-wavelength was necessary to reliably resolve two areas of differing stiffness.

The calculated wavelengths were averaged across the image and then normalized to 100 Hz. The mean Young's modulus-wall thickness products were calculated using the following expression, which was developed previously (10)

$$Et = 2\rho a_i \lambda^2 f^2.$$

where E is the Young's modulus, t is the wall thickness of the aorta, a_i is the interior aorta radius, ρ is the density of the interior fluid, λ is the wavelength, and f is the frequency of dynamic excitation.

Histologic and morphometric analyses

Hematoxylin-and-Eosin (H&E), Elastica-van-Gieson (EvG), and Sirus-Red staining of cross-section of aortic tissue samples, 5 μm in thickness, were performed as previously reported (16,19). Using a digital image system (Nikon DXM 1200; Camera), morphometric analyses on EvG-stained slides were carried out for the assessment of lumen area, internal elastic lamina (IEL) area, and external elastic lamina (EEL) area at a magnification of 10×. Intima area was calculated as IEL area minus lumen area and media area as EEL area minus IEL area, allowing calculation of the intima-media ratio. Intima thickness was calculated as IEL radius minus lumen radius and media thickness as EEL radius minus IEL radius.

Elastin content of the aortic wall was quantified on EvG-stained slides using Meta Imaging Series 4.6 (MetaMorph, Universal Imaging Corporation, Downingtown, PA, USA) and expressed as percentage of total surface area (14,17). In similar technique, collagen content was quantified on Sirus-Red-stained slides.

Statistical analysis

Continuous data were expressed as mean ± standard deviation. Two group comparisons were performed using Student's t-test. Statistical significance was accepted for $p<0.05$.

Results

As expected and outlined in Table 1, mean arterial pressure was higher in hypertensive than in control animals. Animal weight and total cholesterol concentrations were not significantly different (Table 1).

The propagating wave images were well visualized in the aortas from both the control and the hypertensive group (Fig. 1a and b). From these images, quantitative analyses demonstrated a significant increase in the Young's modulus-wall thickness (E*t) product of the hypertensive aortas compared to the controls (0.571 ± 0.080 vs. 0.419 ± 0.026 kPa-m, $p<0.05$) (Fig. 1c).

Aorta segments from control and hypertensive animals were analyzed morphometrically on EvG-stained slides. In hypertensive aortas, there was an increased intima (Table 2) and media thickness (Table 2). Calculation of the intima-media thickness ratio showed no changes between control and hypertensive aortas (Table 2). Area measurements demonstrated similar changes (Table 2). From the wall thickness values and the E*t product, the Young's modulus could be calculated and demonstrated a decrease in the hypertensive aortas (Table 2).

The Sirius Red staining demonstrated a significantly higher collagen content in the hypertensive aortas versus the controls (40.14 ± 3.23 vs. control 26.95 ± 5.25 % aortic wall area) (Fig. 2a and c), especially within the adventitia at the junction to the media. EvG-staining showed no change in the elastin content of the controls (hypertensive 38.99 ± 6.59 vs. control 35.79 ± 4.04 % aortic wall area) (Fig. 2b and d).

Discussion

This phase contrast MRI technique can visualize harmonic mechanical excitations in the aortic wall. With this technique, differences between normal and hypertensive animals can be assessed even in short periods of hypertension. To analyze what this technique is measuring, histological analysis of the aortas reveals near doubling of the wall thickness and increasing collagen density, while the intima-media ratio is unchanged. These findings correlate with symmetrical increases in the intima and media thickness in hypertensive aortas as well as increasing collagen content.

The E*t product significantly increases in hypertensive aortas. This increase could be a reflection of the increasing wall thickness or could be secondary to changing Young's modulus and wall thickness. Calculation of the Young's modulus showed a decrease in hypertensive aortas. The decreasing Young's modulus may reflect the manner in which the aortas were studied. We examined our aortas under isobaric conditions with the same luminal pressure for control and hypertensive aortas. Several studies have shown that comparison of arterial wall elasticity under isobaric conditions can demonstrate decreasing Young's modulus in hypertensive subjects (20,21). Their explanation for this finding is that the Young's modulus is measured at a lower point on the compliance-pressure curve for the hypertensive subject versus the control subject (20,21).

Collagen measurements in normal and hypertensive aortas show a doubling in collagen density in hypertensive aortas, while elastin content is unchanged between the two groups.

Thus, in this animal model of early hypertension, two major changes are occurring in wall thickness and collagen content. These two factors contribute to changing the E*t product which can be quantitated using this phase contrast MRI-based technique. Therefore, the E*t product measurement may more accurately assess changing wall characteristics occurring in early hypertension by taking into account both parameters.

In conclusion, this study demonstrated use of a phase contrast MRI technique to visualize differences in ex-vivo aortic wall stiffness in a porcine model of hypertension. The methodology offers a potentially non-invasive method for early evaluation of the arterial wall mechanical properties without disruption or invasion of the artery itself. However, further investigation is needed on in-vivo arteries. The results do support the hypothesis that subtle changes in arterial elasticity are initiated even during short (3 months) periods of hypertension. Furthermore, these changes can be detected and quantified using this phase contrast MRI-based elastography technique. This would enable the ability to directly monitor the primary organ (vascular wall) damage to aid in therapeutic treatment assessment and possibly study whether arterial wall changes can be reversed in-vivo. The limitations of this study include the use of ex-vivo aortic tissue, use of porcine rather than human arteries, and the fact that measurements were obtained in isobaric conditions. Further investigation will include examination of in-vivo arteries to assess its sensitivity and ultimately study progressive arterial wall elasticity changes in the hypertensive animals.

Acknowledgments

Grant Support: This research was supported by Grants #EB001981 and DK73608.

References

1. Kim EJ, Park CG, Park JS, et al. Relationship between blood pressure parameters and pulse wave velocity in normotensive and hypertensive subjects: invasive study. J Hum Hypertens. 2007; 21(2): 141–148. [PubMed: 17136108]
2. London GM, Guerin AP. Influence of arterial pulse and reflected waves on blood pressure and cardiac function. Am Heart J. 1999; 138(3 Pt 2):220–224. [PubMed: 10467216]
3. Oliver JJ, Webb DJ. Noninvasive assessment of arterial stiffness and risk of atherosclerotic events. Arterioscler Thromb Vasc Biol. 2003; 23(4):554–566. [PubMed: 12615661]
4. Nichols WW. Clinical measurement of arterial stiffness obtained from noninvasive pressure waveforms. Am J Hypertens. 2005; 18(1 Pt 2):3S–10S. [PubMed: 15683725]
5. Woodman RJ, Watts GF. Measurement and application of arterial stiffness in clinical research: focus on new methodologies and diabetes mellitus. Med Sci Monit. 2003; 9(5):RA81–89. [PubMed: 12761466]
6. London GM, Cohn JN. Prognostic application of arterial stiffness: task forces. Am J Hypertens. 2002; 15(8):754–758. [PubMed: 12160201]
7. Woodrum DA, Romano AJ, Lerman A, et al. Vascular wall elasticity measurement by magnetic resonance imaging. Magn Reson Med. 2006; 56(3):593–600. [PubMed: 16902974]
8. Muthupillai R, Lomas DJ, Rossman PJ, Greenleaf JF, Manduca A, Ehman RL. Magnetic resonance elastography by direct visualization of propagating acoustic strain waves. Science. 1995; 269(5232): 1854–1857. [PubMed: 7569924]
9. Draney MT, Arko FR, Alley MT, Markl M, Herfkens RJ, Pelc NJ, Zarins CK, Taylor CA. Quantification of vessel wall motion and cyclic strain using cine phase contrast MRI: In vivo validation in the porcine aorta. Magn Reson Med. 2004; 52(2):286–295. [PubMed: 15282810]
10. Muthupillai R, Rossman PJ, Lomas DJ, Greenleaf JF, Riederer SJ, Ehman RL. Magnetic resonance imaging of transverse acoustic strain waves. Magn Reson Med. 1996; 36(2):266–274. [PubMed: 8843381]

11. Romano AJ, Abraham PB, Rossman PJ, Bucaro JA, Ehman RL. Determination and analysis of guided wave propagation using magnetic resonance elastography. Magn Reson Med. 2005; 54(4): 893–900. [PubMed: 16155879]
12. Leveson SH, Guillou PJ, Terry HJ, Glanville JN, Kester RC. Pulse pressure wave analysis in the diagnosis of aorto-iliac disease. Ann Surg. 1978; 187(2):161–165. [PubMed: 629617]
13. Lerman LO, Schwartz RS, Grande JP, Sheedy PF, Romero JC. Noninvasive evaluation of a novel swine model of renal artery stenosis. J Am Soc Nephrol. 1999; 10(7):1455–1465. [PubMed: 10405201]
14. Herrmann J, Samee S, Chade A, Rodriguez Porcel M, Lerman LO, Lerman A. Differential effect of experimental hypertension and hypercholesterolemia on adventitial remodeling. Arterioscler Thromb Vasc Biol. 2005; 25(2):447–453. [PubMed: 15591225]
15. Chade AR, Rodriguez-Porcel M, Grande JP, et al. Mechanisms of renal structural alterations in combined hypercholesterolemia and renal artery stenosis. Arterioscler Thromb Vasc Biol. 2003; 23(7):1295–1301. [PubMed: 12750121]
16. Callaghan PT, Stepisnik J. Frequency-Domain Analysis of Spin Motion Using Modulated-Gradient NMR. J Magn Reson. 1995; 117:118–122.
17. Versari D, Herrmann J, Gossl M, et al. Dysregulation of the ubiquitin-proteasome system in human carotid atherosclerosis. Arterioscler Thromb Vasc Biol. 2006; 26(9):2132–2139. [PubMed: 16778122]
18. Manduca A, Lake DS, Kruse SA, Ehman RL. Spatio-temporal directional filtering for improved inversion of MR elastography images. Med Image Anal. 2003; 7:465–473. [PubMed: 14561551]
19. Pannier BM, Avolio AP, Hoeks A, Mancia G, Takazawa K. Methods and devices for measuring arterial compliance in humans. Am J Hypertens. 2002; 15(8):743–753. [PubMed: 12160200]
20. Van Bortel LM, Duprez D, Starmans-Kool MJ, et al. Clinical applications of arterial stiffness, Task Force III: recommendations for user procedures. Am J Hypertens. 2002; 15(5):445–452. [PubMed: 12022247]
21. Riley WA, Evans GW, Sharrett AR, Burke GL, Barnes RW. Variation of common carotid artery elasticity with intimal-medial thickness: the ARIC Study. Atherosclerosis Risk in Communities. Ultrasound Med Biol. 1997; 23(2):157–164. [PubMed: 9140173]

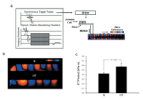

Figure 1.
Representative images from phase contrast MRI-based elastography in ex vivo porcine aortas. a: Schematic of a gradient-echo pulse sequence with an additional transient motion-encoding gradient. By varying the phase offset, θ, the propagating wave is captured along the length of the vessel. The electromechanical impulse generator is shown in contact with the aortic wall. b: Propagating mechanical waves demonstrated within an ex-vivo porcine abdominal aorta. The signal intensity on the wave images represents the displacement amplitude at equally spaced intervals in one wave cycle. Wave propagation is away from the driver in the left–right direction. Signal intensity decreases with increasing propagation distance due to attenuation. c: The (E*t) product is calculated from the propagating wave. Hypertensive animals have a significantly higher (E*t) product versus control. * Denotes statistically significance difference by comparison Student's t-test with $p<0.05$ being significant.

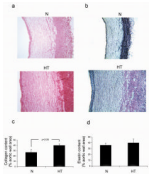

Figure 2.

Assessment of collagen and elastin content in the aortic wall of control (N) and hypertensive (HT) aortas. a: Sirius Red staining demonstrates dense collagen deposition in the adventitia in HT and especially at the junction to the media. Magnification is 10×. b: Elastica-van - Gieson staining elastin fibers within the aortic wall. Magnification is 10×. c: Quantification of the Sirius Red shows increased collagen density within the hypertensive aortas. d: Quantification of the elastin staining shows no difference between normal and hypertensive aortas. Statistical comparison performed with Student's t-test with $p<0.05$ being significant.

TABLE 1

Mean Arterial Pressure (MAP), Weight, and Total Cholesterol in Control (N) and Hypertensive (HT) Pigs.

	Control (N)	Hypertensive (HT)
Mean Arterial Pressure	115 ± 11	173 ± 12*
Weight	53 ± 10	56 ± 7
Total Cholesterol	74 ± 15	77 ± 15

* $p \leq 0.05$ vs. normal (values ± standard deviation)

TABLE 2

Histologic Morphometric Analysis results from control (N) and hypertensive (HT) aortas. Young's modulus was calculated using the combined intima-media thickness.

	Control (N)	Hypertensive (HT)	P-Value
Intima area [mm^2]	0.135 ± 0.041	0.378 ± 0.106	0.001
Media area [mm^2]	4.536 ± 0.752	12.535 ± 1.264	<0.001
Ratio intima/media area	0.029 ± 0.005	0.031 ± 0.011	0.781
Lumen radius [mm]	1.233 ± 0.170	1.922 ± 0.190	<0.001
Intima radius [mm]	1.250 ± 0.017	1.953 ± 0.185	<0.001
Media radius [mm]	1.733 ± 0.179	2.739 ± 0.179	<0.001
Intima thickness [mm]	0.017 ± 0.005	0.032 ± 0.010	0.02
Media thickness [mm]	0.483 ± 0.048	0.841 ± 0.059	<0.001
Intima+media thickness [mm]	0.501 ± 0.053	0.873 ± 0.053	<0.001
Ratio intima/media thickness	0.036 ± 0.014	0.038 ± 0.007	0.719
Young's Modulus [×10^5 Pa]	8.53 ± 1.05	6.06 ± 1.36	<0.001

Values are mean ± standard deviation.